

## Research Article

# Estimation of Suspended Sediment Load Using Artificial Intelligence-Based Ensemble Model

Vahid Nourani <sup>1</sup>, Huseyin Gokcekus <sup>2</sup>, and Gebre Gelete <sup>2,3</sup>

<sup>1</sup>Center of Excellence in Hydroinformatics and Faculty of Civil Engineering, University of Tabriz, Tabriz, Iran

<sup>2</sup>Faculty of Civil and Environmental Engineering, Near East University, Northern Cyprus, Mersin 10, Turkey

<sup>3</sup>College of Agriculture and Environmental Science, Arsi University, 193, Asela, Ethiopia

Correspondence should be addressed to Vahid Nourani; [vnourani@yahoo.com](mailto:vnourani@yahoo.com)

Received 13 December 2020; Revised 15 January 2021; Accepted 5 February 2021; Published 17 February 2021

Academic Editor: Haitham Afan

Copyright © 2021 Vahid Nourani et al. This is an open access article distributed under the Creative Commons Attribution License, which permits unrestricted use, distribution, and reproduction in any medium, provided the original work is properly cited.

Suspended sediment modeling is an important subject for decision-makers at the catchment level. Accurate and reliable modeling of suspended sediment load (SSL) is important for planning, managing, and designing of water resource structures and river systems. The objective of this study was to develop artificial intelligence- (AI-) based ensemble methods for modeling SSL in Katar catchment, Ethiopia. In this paper, three single AI-based models, that is, support vector machine (SVM), adaptive neurofuzzy inference system (ANFIS), feed-forward neural network (FFNN), and one conventional multilinear regression (MLR) modes, were used for SSL modeling. Besides, four different ensemble methods, neural network ensemble (NNE), ANFIS ensemble (AE), weighted average ensemble (WAE), and simple average ensemble (SAE), were developed by combining the outputs of the four single models to improve their predictive performance. The study used two-year (2016-2017) discharge and SSL data for training and verification of the applied models. Determination coefficient (DC) and root mean square error (RMSE) were used to evaluate the performances of the developed models. Based on the performance measure results, the ANFIS model provides higher efficiency than the other developed single models. Out of all developed ensemble models, the nonlinear ANFIS model combination method was found to be the most accurate method and could increase the efficiency of SVM, MLR, ANFIS, and FFNN models by 19.02%, 37%, 9.73%, and 16.3%, respectively, at the verification stage. Overall, the proposed ensemble models in general and the AI-based ensemble in particular provide excellent performance in SSL estimation.

## 1. Introduction

Accurate modeling of the suspended sediment transported by a river is of great importance in environmental and water resources engineering, as it directly affects the design, planning, operation, and management of water resources [1]. Moreover, modeling of suspended sediment is crucial because it has a major effect on the reservoir capacity and dam operation [2], water quality, and contaminant transport [3, 4]. However, suspended sediment estimation is a challenging task for hydrologists as its interaction with geomorphological characteristics of the catchment and the streamflow is highly complex and nonlinear. Suspended sediment transport in the river is a function of meteorological and hydrological parameters as a complicated process [5].

For the last decades, several studies were conducted to model the relationship between river flow and suspended sediment amount [1]. However, none of the developed models has gotten universal acceptance for application in all cases. So far, several researchers have proposed many models to estimate this complex process ranging from simple statistical, physical, and black-box models. In earlier decades, modeling suspended sediment load using mathematical models was a common task. However, their application was limited because of the significant time required to set up the model [6] and the large number of variables involved in the equations [7].

The physically based models are reliable methods for assessing the actual physics of a phenomenon. Physically based models for suspended sediment load (SSL) modeling

are usually based on the simplified equation of sediment and discharge as well as on the relationship between the erosive effect of flow and rainfall (e.g., [8–10]). Such physical and conceptual models can take into account the effect of catchment property and uneven distribution evapotranspiration and rainfall on the catchment [1]. However, using physically based models for hydrological modeling is rather complex as they require detailed temporal and spatial data, which are not easily available. Estimating suspended sediment load using a physically based model is a very difficult task due to its requirement of high-resolution sediment and discharge data which are not often available [11]. Moreover, direct measurement of high-resolution sediment concentration and discharge is expensive and any error in measurement of these variables also influences the modeling of suspended sediment load. When accurate estimation is more important than the physical understanding of the phenomenon, the application of black-box modeling is helpful.

To overcome the limitation of the physical-based models, black-box artificial intelligence- (AI-) based approaches which are reliable methods in dealing with nonlinear and complex phenomena have been employed in different fields of water resources engineering. Examples of this include modeling suspended sediment load of the rivers (e.g., see [12, 13]), rainfall-runoff process (e.g., see [14, 15]), longitudinal dispersion coefficient of water pipeline (e.g., see [16]), and estimation of overtopping flow the incipient motion of riprap stones (e.g., see, [17]). The AI methods applied for the modeling of SSL include artificial neural network (ANN), adaptive neurofuzzy inference system (ANFIS), and support vector machine (SVM). ANFIS model is an AI-based model appropriate for modeling nonlinear and complex processes like suspended sediment load (e.g., [1, 12–18]). So far, different works have been reported in the literature on the application of ANN in SSL modeling (e.g., [19–21]). SVM is another AI-based model capable of giving a reliable estimation of suspended sediment load (e.g., [1, 4, 22]). In addition to AI-based models, conventional multilinear regression (MLR) was used in this study. Because of some difficulties in working with AI-based models, some researchers applied straightforward, simple, and fast modeling tools such as MLR to describe the linear relationship between the response and one or more independent variables [23]. MLR has been successfully applied in modeling different hydrological problems like evapotranspiration [23], rainfall-runoff process [14], and suspended sediment load [20, 24].

Although the abovementioned AI-based models can give reasonable results, it is clear that one model may show higher performance than the others for a given data set and when different data sets are used, the results may entirely be different [25]. No single model is superior in providing a hydrological process forecast for any kind of watershed in all conditions compared to those of other competing models [26]. Therefore, combining the outputs of different models using different ensemble techniques was believed to give high predictive performance results and low error by taking the advantages of different models. In this regard, Bates and Granger [27] approved that combining the

outputs from several models using ensemble techniques would lead to results that outperform the individual forecasts. The thought behind the model combination is to make use of the exclusive characteristics of the single models in a unique framework that would improve the modeling accuracy [28]. The combination of different model outputs using several ensemble techniques has become a common practice for the improvement of prediction accuracy in different fields [29–31]. In the field of hydrology, the first ensemble method was examined by Cavadias and Morin [32]. Since then, the advantages of ensemble techniques for improving modeling efficiency have been proven in modeling several hydrological processes (e.g., see [26, 33, 34]). However, to date and based on our knowledge, there is no study done so far showing the application of AI-based model combination methods for suspended sediment load simulation. The main objective of this work was to develop AI-based ensemble methods for daily suspended sediment load estimation in Katar catchment, Ethiopia. Three steps were followed to achieve this objective. Sensitivity analysis was made to select significant and relevant inputs in the first step. Secondly, four black-box models, namely, ANFIS, ANN, SVM, and MLR models, were developed to estimate suspended sediment load. These AI-based (ANFIS, FFNN, and SVM) models are chosen in this study because of their fast convergence time, simplicity, and reliable estimation performance for complex hydrological processes like SSL. Finally, the four ensemble models (ANFIS ensemble (AE), neural network ensemble (NNE), simple average ensemble (SAE), and weighted average ensemble (WAE)) were created to increase the predicting performance of the single black-box models in forecasting suspended sediment. AE and NNE were chosen as the nonlinear ensemble method over the other AI-based models because of their compatibility, popularity, and also their high performance reported in model combination studies in other different fields [25, 35]. Moreover, the AE was introduced in this study due to the robustness of the model observed in the single models. These ensemble techniques have the potential to provide researchers, decision-makers, and river and watershed managers with accurate and fast methods for SSL estimation.

The models were examined for modeling SSL of Katar catchment containing Katar River that drains into Lake Ziway which supports the lives of millions of people. The catchment is characterized by intensive agriculture where both rainfed and irrigated crops are grown. Because of sediment deposition attributed to periodic flooding together with improper agriculture, floodplains are formed along the bank of the lake and the river. Moreover, this sediment transported through the river causes siltation of irrigation canals and Lake Ziway. Thus, in this study, the Katar catchment is chosen as the case study due to the availability of discharge and SSL data (even though it is only two years) and also for challenging problems associated with sedimentation. Therefore, the Katar catchment represents a good case study to assess the SSL estimation accuracy of the proposed single and ensemble models.

## 2. Materials and Methods

**2.1. Study Area Description.** The study area, the Katar River catchment, is a subcatchment of the Ethiopian central rift valley basin. This watershed is located in the Oromia Regional State of Ethiopia and the northern part of the central rift valley basin as part of the Ziway-Shala basin. Geographically, the catchment lies between 7°21'34" and 8°9'55" north latitudes and 38°53'57" and 39°24'46" east longitude (see Figure 1). The topography of the Katar catchment is complex, with elevations ranging from 1673 m (Abura) to 4181 m above sea level. The total area of the watershed, upstream, of the Abura gauging station is estimated to be 3350 km<sup>2</sup>. The climate of the catchment is characterized by a semiarid to subhumid climate with minimum and maximum annual precipitation values of 731.8 mm and 1229.7 mm, respectively. The mean annual temperature ranges between 16°C and 20°C. The dry season occurs from October to May, and more than 70% of the rain falls during the summer season. The catchment attained a maximum discharge of 116.32 m<sup>3</sup>/s in August and a minimum discharge of 0.115 m<sup>3</sup>/s in January. Runoff from Katar catchment drains into the Lake Ziway. The land use of the study area is characterized dominantly by intensive agriculture where both rainfed and irrigated crops are grown.

Regarding soil type, Katar catchment consists of six major soil types as vertisols, andosols, leptosols, fluvisols, cambisols, and luvisols (see Figure 2).

**2.1.1. Sedimentation Problem in the Study Area.** Katar catchment is one of the data-scarce areas of the country where there is very limited historical measured suspended sediment data. Therefore, studying suspended sediment of the catchment is important to obtain accurate information about the siltation rate and the resulted reservoir storage loss over time. The catchment attains a maximum SSL of 57335.524 ton/day in August and a minimum SSL of 0 ton/day in January. The catchment is one of the degraded areas with intensive agriculture and farming on steep slopes. Furthermore, the dense population together with improper agricultural activity and rolling topography makes the catchment susceptible to soil erosion. The Katar River joins Lake Ziway and according to Aga et al. [36], there is a proposed dam on this river for multiple uses. Soil erosion due to poor management and heavy rainfall is common phenomena occurring upstream. The sediment is transported and deposited at the mouth of the stream channel (see Figure 3). Despite the aforementioned problems, little attention was given to the catchment in the field of suspended sediment load modeling and management. Therefore, it is necessary to study the SSL of the catchment using an effective technique to obtain better information about the sediment condition of the area to have reliable management projects.

**2.2. Data Used in the Study.** In this study, the daily SSL and discharge data of Katar River catchment at Abura station for two years (2016–2017) were used for training and verification

of the developed models. The data were divided into two subsets: the first 70% were used for training and 30% of the data were used for verification purposes. Table 1 presents the descriptive statistics (minimum, average, maximum, and standard deviation) of the used data.

The time series plot of daily SSL and discharge values of Katar catchment at Abura station throughout the study period is shown in Figure 4. The data from 1 January 2016 to 25 May 2017 were used for training and the remaining data (from 26 May to 31 December 2017) served for verification of the applied models.

**2.3. Proposed Methodology.** In this paper, three AI (SVM, ANFIS, and FFNN) and one MLR were used for modeling suspended sediment load in the Katar catchment. The input data used were normalized and classified into training and verification sets. The study was conducted via three stages (see Figure 5). In the first stage, the selection of the most relevant and dominant inputs for suspended sediment load estimation was conducted through nonlinear sensitivity analysis. Secondly, four black-box models, namely, FFNN, SVM, NFIS, and MLR, models were applied for the estimation of suspended sediment. Finally, four ensemble techniques, namely, AE, NNE, SAE, and WAE, were developed. In this stage, the outputs from single black-box models were used as the inputs for the ensemble process. The obtained suspended sediment load from the last stage was compared with the results obtained from individual models in the second step.

**2.3.1. Feed-Forward Neural Network (FFNN).** ANN is among the extensively applied AI techniques in hydrological modeling which works based on simulation of the structure and operational performance of a biological neural network. In recent years, ANN as a self-adaptive and self-learning simulation function has shown great ability in forecasting and modeling complex hydrological processes. Its ability to learn from example makes ANN more efficient and applicable in many fields of science, economics, engineering, etc. [35]. According to [37], the advantage of the ANN model is that it establishes a relationship between the dependent and predicted variables by training the neural network without detailed knowledge of the characteristics of the catchment. Among different ANN forms, FFNN with a backpropagation algorithm was used for this study because of its simplicity and extraordinary preferred position of giving exceptional answers for different problems without prior knowledge of the process.

The FFNN consists of interconnected processing elements known as nodes with unique characteristics of information processing such as learning, nonlinearity, noise tolerance, and generalization capability.

FFNN structure contains three layers, namely, the input, hidden, and output layer (see Figure 6). In the FFNN, the inputs presented to the input layers' neuron are propagated in a forward direction and a nonlinear function known as activation function is used to compute the output vector.

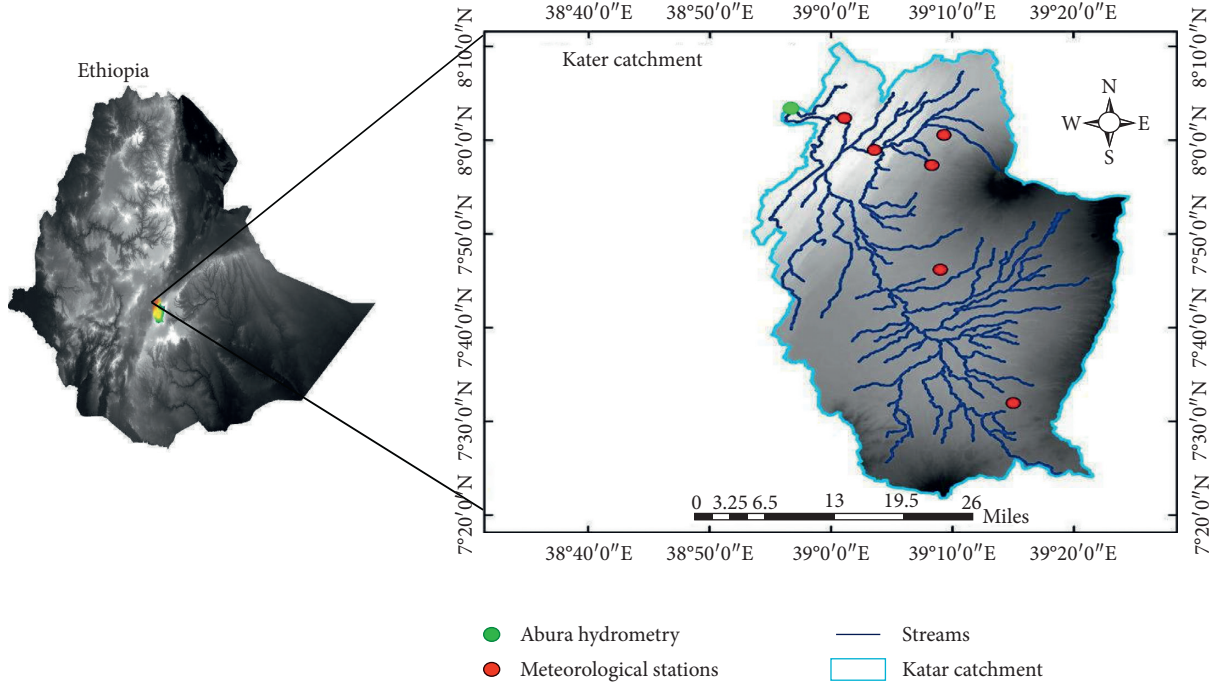


FIGURE 1: Study area map.

**2.3.2. Adaptive Neurofuzzy Inference System (ANFIS).** ANFIS developed by Jang [38] is a universal approximator to overcome the limitations of both ANN and fuzzy inference system. ANFIS is an amalgamation of both ANN and fuzzy inference systems (FIS) that has a strong capability to handle the uncertainty of dynamic and complex interactions that exist between the input and output variables.

Every fuzzy system has three different parts, namely, defuzzifier, fuzzifier, and fuzzy database. The fuzzy rule base consists of rules which are fuzzy proposition related as is demonstrated by Jang et al. [39]. As a result, the fuzzy inference is applied in the operational analysis. This goal can be achieved by employing different fuzzy inference engine. The most famous FIS are Tsukamoto's system [40], Sugeno's system [41], and Mamdani's system [42]. These three types are different from each other. Sugeno's approach uses constant functions, whereas fuzzy membership functions (MFs) are used in Mamdani's approach.

The ANFIS model architecture consists of five layers with layer 1 representing the input layer; layer 2 representing the input membership function; layer 3 representing rules; layer 4 representing the output MFs; and layer 5 representing the output configured as illustrated in Figure 7.

Once the fuzzy system has been built, the relation between fuzzy variables is specified using if-then fuzzy rules. Assuming that FIS contains two inputs ( $x$  and  $y$ ) and output ( $f$ ), a first-order Sugeno fuzzy has the following rules:

Rule (1): if  $\mu(x)$  is  $A_1$  and  $\mu(y)$  is  $B_1$ : then  $f_1 = p_1x + q_1y + r_1$ ,

Rule (2): if  $\mu(x)$  is  $A_2$  and  $\mu(y)$  is  $B_2$ : then  $f_2 = p_2x + q_2y + r_2$ ,

(1)

where  $A_1$  and  $A_2$  are MF parameters for input  $x$  and  $B_1$  and  $B_2$  are MFs for the inputs  $y$ , respectively, whereas  $p_1, q_1, r_1, p_2, q_2,$  and  $r_2$  are outlet functions' parameters. The arrangement and structural formula of ANFIS layers are as follows:

Layer 1: every node  $i$  is an adaptive node in this layer, which has a node function as equation (2).

$$Q_i^1 = \mu A_i(x), \quad \text{for } i = 1, 2$$

$$\text{or } Q_i^1 = \mu B_i(x), \quad \text{for } i = 3, 4, \quad (2)$$

where  $Q_i^1$  represents the membership grade for inputs  $x$  and  $y$ . Gaussian MF was chosen due to its lowest prediction error.

Layer 2: every rule between inputs in this layer is connected by the T-Norm operator which is performed with "and" operator as in equation (3).

$$Q_i^2 = w_i = \mu A_i(x) \cdot \mu B_i(y), \quad \text{for } i = 1, 2. \quad (3)$$

Layer 3: the output in this layer is normalized firing strength and calculated as

$$Q_i^3 = \bar{w} = \frac{w_i}{w_1 + w_2}, \quad i = 1, 2. \quad (4)$$

Layer 4: each node  $i$  in this layer calculates the consequence of the rules on the output of the model:

$$Q_i^4 = \bar{w}(p_i x + q_i y + r_i) = \bar{w} f_i. \quad (5)$$

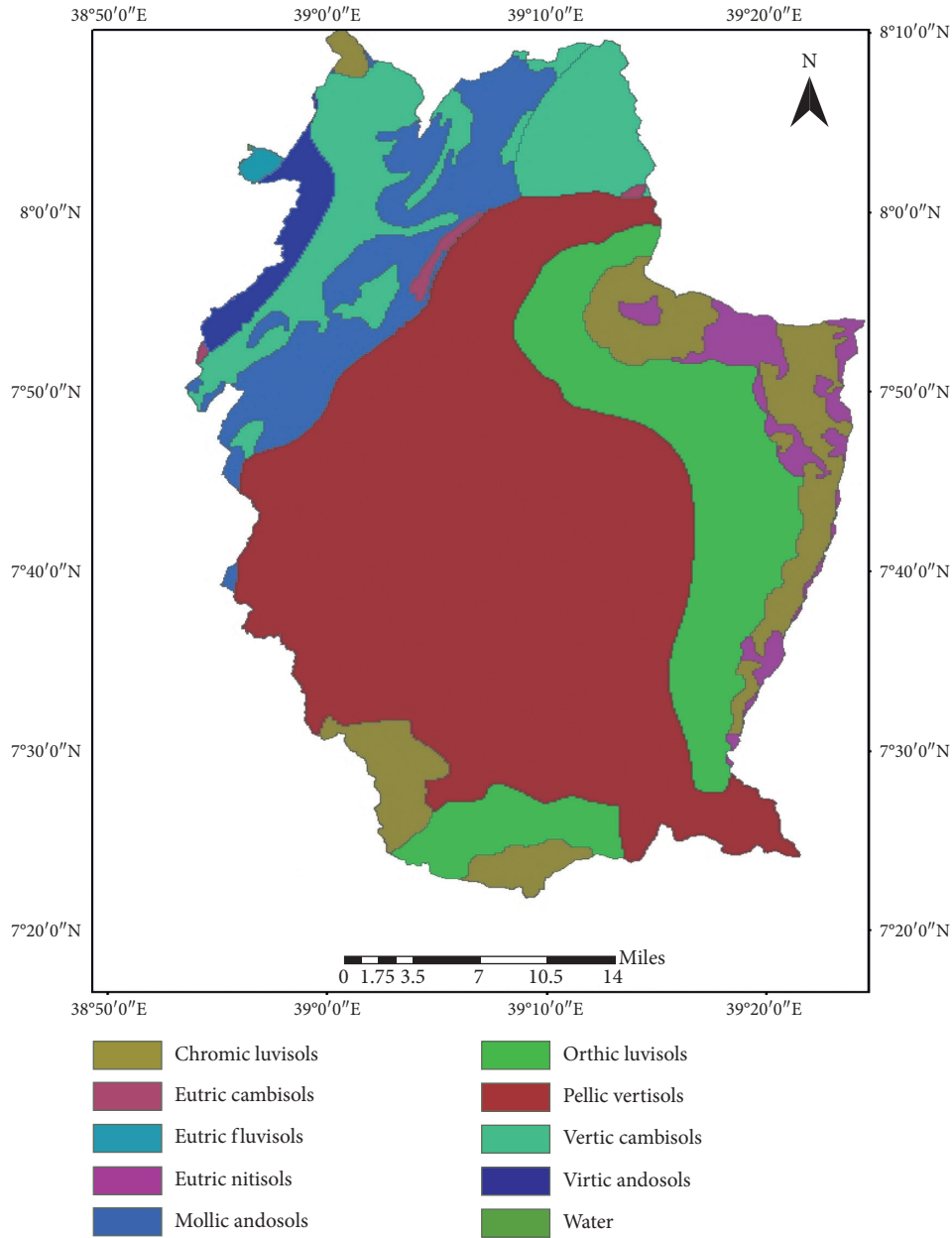


FIGURE 2: Soil map of the study area.



FIGURE 3: Siltation along the riverbank [36].

$\bar{w}$  is the layer 3 output and  $p_1$ ,  $q_1$ , and  $r_1$  are consequent parameters.

Layer 5: the overall ANFIS output is calculated by adding all of the incoming signals to this layer as

$$Q_i^5 = \bar{w}(p_i x + q_i y + r_i) \sum w_i f_i = \frac{\sum w_i f_i}{\sum w_i} \quad (6)$$

2.3.3. *Support Vector Machine (SVM)*. It is an artificial intelligence model that can be used for both regression and classification tasks [43]. SVM is a relatively new approach that can successfully be applied in the modeling of nonlinear

TABLE 1: Descriptive statistics of daily runoff and sediment data.

Data set	Period	Statistical parameters				
		Min	Mean	Max	Standard deviation	Coefficient of variation
Discharge (m <sup>3</sup> /s)	Training	0.115	8.862	116.32	15.3016	1.727
	Verification	0.8	17.338	111.32	20.062	1.157
	Whole	0.115	11.401	116.32	17.31	1.518
SSL (ton/day)	Training	0	1760.29	57335.524	5102.626	2.899
	Verification	0	3391.356	52947.35	5850.01	1.725
	Whole	0	2248.94	57335.52	5389.566	2.397

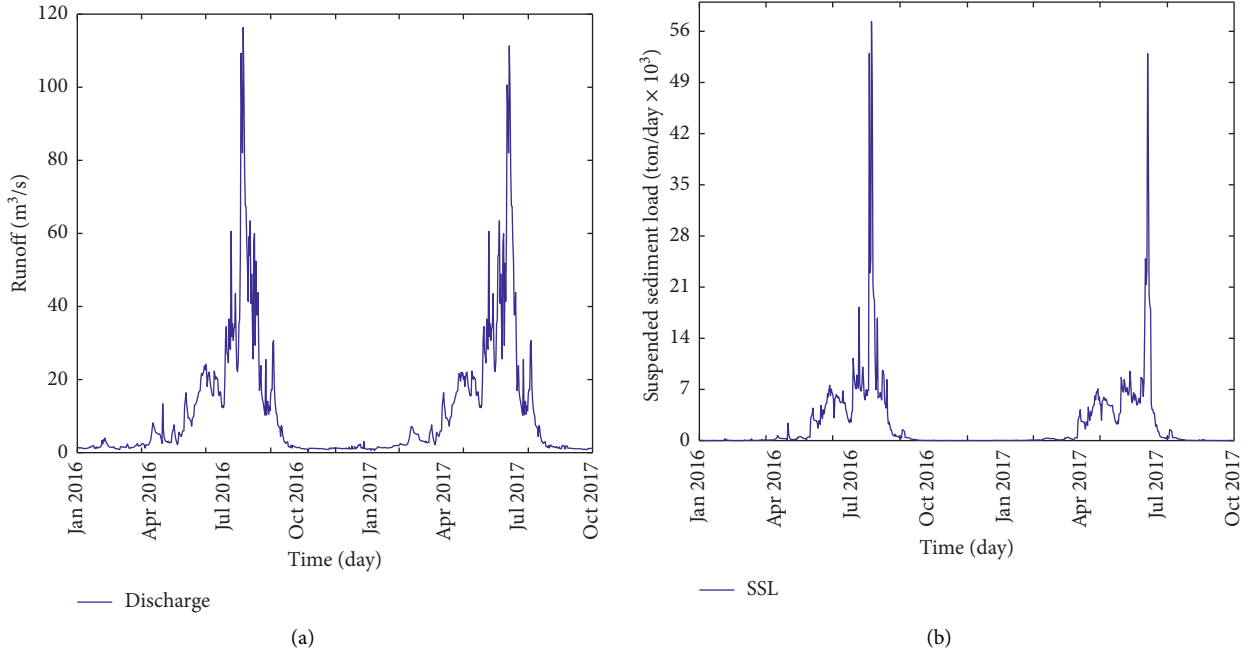


FIGURE 4: Time series of suspended sediment load and river discharge observed at Katar catchment (Abura station) for a period of two years (2016-2017).

and complex real-world problems. The regression estimation with SVM is to estimate a function according to a given data set,  $\{(x_i, d_i)\}_i^n$  where  $x_i$  denotes the input vector,  $d_i$  denotes the actual value, and  $n$  is the total number of data sets. The general SVM regression function is formulated as

$$y = f(x) = \omega\phi(x_i) + b, \quad (7)$$

where  $\phi$  is nonlinear mapping function and  $\omega$  and  $b$  are regression function parameters and determined by assigning positive values for the slack parameters of  $\xi$  and  $\xi^*$  and minimization of the objective function as shown in

$$\begin{aligned} & \text{Minimize } \frac{1}{2}\|w\|^2 + c \left( \sum_i (\xi_i + \xi_i^*) \right) \\ & \text{Subjected to } \begin{cases} \omega_i\phi(x_i) + b_i - d_i \leq \varepsilon + \xi_i^* \\ d_i - \omega_i\phi(x_i) + b_i \leq \varepsilon + \xi_i \\ \xi_i, \xi_i^* \end{cases}, \quad i = 1, 2, \dots, n, \end{aligned} \quad (8)$$

where  $(1/2)\|w\|^2$  is the weights vector norm and  $C$  is the regularized constant; the general conceptual model structure of SVM is illustrated in Figure 8.

By defining Lagrange multipliers  $\alpha_i$  and  $\alpha_i^*$ , the optimization problem shown above can be changed to a dual quadratic optimization problem. The vector  $w$  can be determined after finding the problem solution of optimization [44].

$$w^* = \sum_i^n (\alpha_i - \alpha_i^*)\phi(x_i). \quad (9)$$

Therefore, the general form of SVM can be in the form as

$$f(x, \alpha_i, \alpha_i^*) = \sum_{i=1}^n (\alpha_i - \alpha_i^*)K(x, x_i) + b, \quad (10)$$

where  $k(x_i, x_j)$  is the kernel function and  $b$  is the bias term. The radial basis function (Gaussian) is the most common kernel function [45] and is expressed as

$$k(x_1, x_2) = \exp\left(-\gamma\|x_1 - x_2\|^2\right), \quad (11)$$

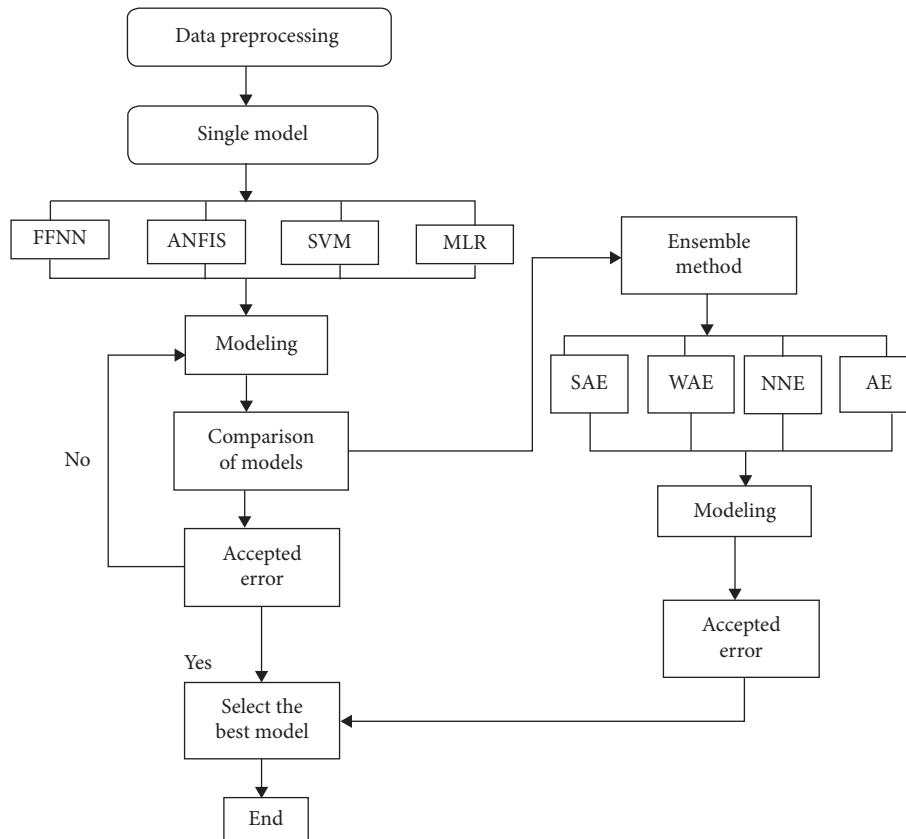


FIGURE 5: Schematic of the proposed methodology.

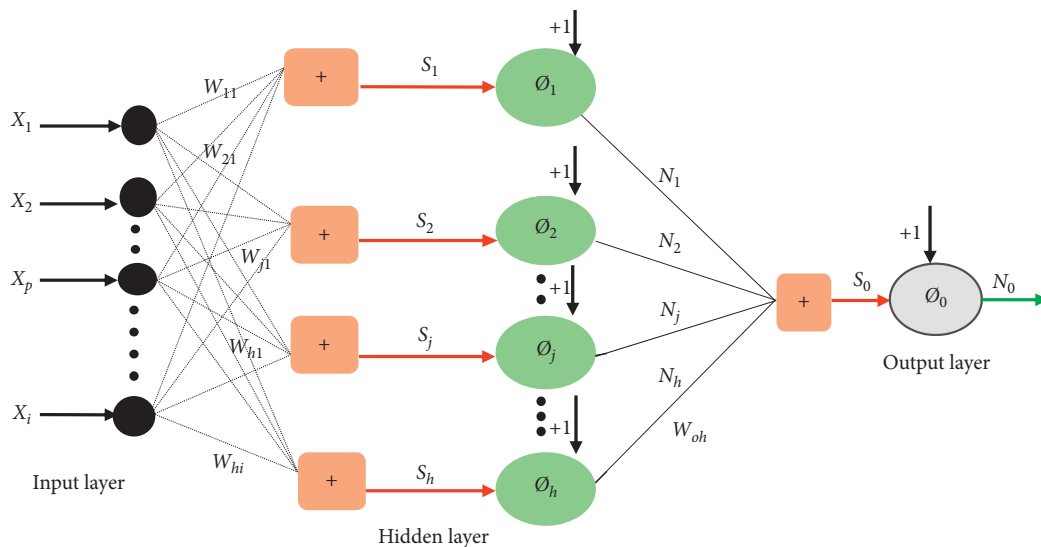


FIGURE 6: The structure of the FFNN model.

where  $\gamma$  is the kernel parameter.

2.3.4. *Multilinear Regression (MLR)*. MLR is one of the most commonly used mathematical modeling techniques to analyze the linear relationship that exists between the

dependent and one or more independent variables. This method is based on the assumption that the dependent variable  $Y$  is affected by predictor variables  $X_1, X_2, \dots, X_n$  and then a linear equation is selected for the relationship between the dependent and independent variables [14].

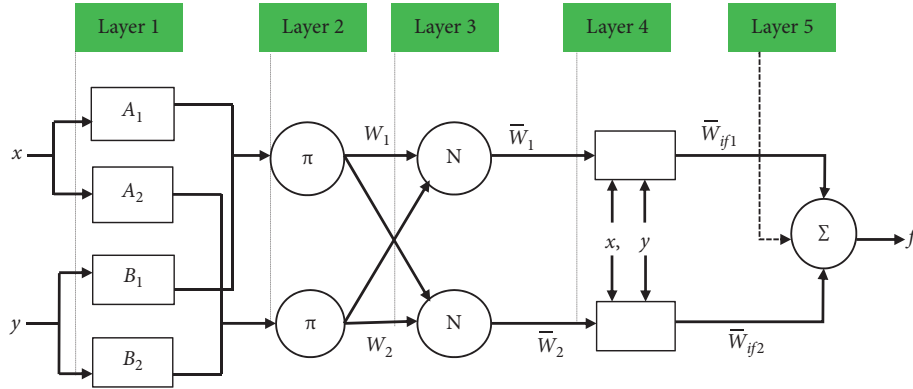


FIGURE 7: Structure of equivalent ANFIS.

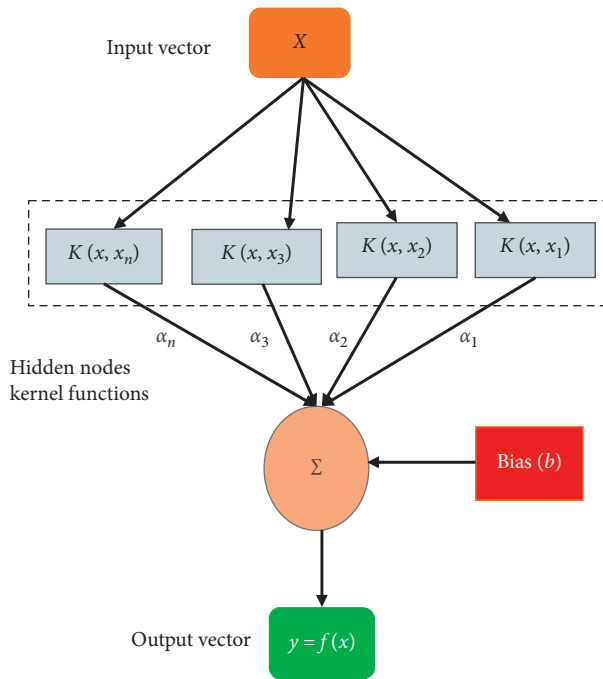


FIGURE 8: The architecture of SVM algorithms.

Generally, the regression equation for the dependent variable ( $Y$ ) can be written as

$$Y = b_0 + b_1x_1 + b_2x_2 + \dots + b_nx_n, \quad (12)$$

where  $x_n$  is the value of the  $n^{\text{th}}$  predictor,  $b_0$  is the regression constant, and  $b_n$  is the coefficient of the  $n^{\text{th}}$  predictor.

**2.4. Ensemble Techniques.** Ensemble modeling is a type of machine learning in which the outputs of different models are combined to improve the final model

performance [46]. Even though it is a complex process and consumes a long time for designing and computation, an amalgamation of the outputs of several models produces results that are more accurate than the individual models [47]. This is because one of the used techniques for a given data set may perform better than the others and when different data sets are used, the result may become the opposite. Therefore, an ensemble technique may be developed to get benefit from the advantages of all single models. Ensemble method utilizes output from every single method with a certain priority level assigned to each with the help of arbitrator, providing the output [28]. For this study, two nonlinear (AE and NNE) and two linear (WAE and SAE) ensemble models were used for enhancing the performance of the single models.

Multimodel combination methods have already been applied in various forecasting applications such as clustering, classification, time series, regression and web ranking [48], weather and economic forecasting in the early 1960s [49], rainfall-runoff [26], dissolved oxygen concentration modeling [50], groundwater level prediction [34], river water quality index prediction [30], and wastewater effluent quality modeling [31]. However, no study is reported on the applicability of ensemble modeling in suspended sediment load modeling to the best of our knowledge. Thus, this study employed four ensemble methods (two nonlinear and two linear) to enhance the accuracy of the single models in the estimation of SSL.

**2.4.1. Linear Ensemble Methods.** Simple average ensemble (SAM): in this ensemble technique, the arithmetic average of outputs (suspended sediment load) of SVM, ANFIS, FFNN, and MLR models was calculated as the final computed suspended sediment load value as



$$SS = \frac{1}{N} \sum_{i=1}^N SS_i, \quad (13)$$

where  $SS$  is the output of the SAM model,  $SS_i$  is the output of the  $i^{\text{th}}$  single model (i.e., ANFIS, FFNN, SVM, and MLR), and  $N$  is the number of single models (here,  $N=4$ ).

Weighted average ensemble (WAE): in this method, the prediction is made by assigning different weight to each output based on the relative importance of the outputs as

$$SS = \sum_{i=1}^N w_i SS_i, \quad (14)$$

where  $w_i$  stands for weight on the output of the  $i^{\text{th}}$  method and it is computed based on the performance measure of the  $i^{\text{th}}$  method as

$$w_i = \frac{DC_i}{\sum_{i=1}^N DC_i}, \quad (15)$$

where  $DC_i$  represents the determination coefficient of the  $i^{\text{th}}$  model.

**2.4.2. Nonlinear Ensemble Methods.** In the nonlinear ensemble methods, the nonlinear averaging is performed by training an AI nonlinear model such as ANFIS and FFNN using suspended sediment values obtained from the single models. In the nonlinear ensemble modeling, the outputs of individual ANFIS, SVM, MLR, and FFNN models are combined and used as new inputs for the nonlinear ensemble models (AE and NNE) to get the overall ensemble output.

Neural network ensemble (NNE): in this technique, a nonlinear ensemble is made by training another FFNN by feeding the outputs of single models as inputs. Then, the maximum number of epochs and hidden layers' neurons is determined by trial and error.

ANFIS ensemble (AE): in this method, the suspended sediment load values obtained from single SVM, FFNN, MLR, and ANFIS models are fed to train a new ANFIS model using various numbers of epochs and membership functions. The general procedure used in the ensemble process is presented in Figure 9.

**2.5. Data Normalization and Model Evaluation Criteria.** The input and output data should be first normalized before the model is trained to remove their dimensions and to ensure that equal attention is given to all variables [25, 47]. Data normalization helps to avoid numerical calculation difficulty. To bring the data in a range of [0, 1], the dataset should be normalized as

$$SS_n = \frac{SS_i - SS_{\min}}{SS_{\max} - SS_{\min}}, \quad (16)$$

where  $SS_n$ ,  $SS_{\max}$ ,  $SS_{\min}$ , and  $SS_i$  represent the normalized, maximum, minimum, and actual suspended sediment load values, respectively.

In forecasting hydrological parameters, Dawson et al. [51] discussed and explained 20 frequently used model performance indicators. As indicated in the previous parts, three AI-based models (ANFIS, ANN, and SVM) and a commonly used linear model (MLR) were used in this study. The performance of hydrological and climatological time series forecasting models must be evaluated in both training and verification phases. The model that yields the best modeling result on the training and verification steps is determined by trial and error. For better evaluation of model performance, at least one absolute error measure and one good of fit should be used [47]. For this study, Root Mean Square Error (RMSE) and Nash-Sutcliffe Efficiency (NSE) or Determination Coefficient (DC) were used to evaluate the performance and efficiency of the developed models. DC has values between  $-\infty$  and 1 and measures how well the predicted value fits with the observed data. Higher model performance is obtained when the DC value is closed to 1, and vice versa [52]. The other performance measure used in this study is RMSE. It measures the deviation of the computed from the observed values. The best model is the model that gives the least RMSE and the highest DC values, as calculated by equations (17) and (18), respectively.

$$RMSE = \sqrt{\frac{1}{N} \sum_{i=1}^N (SS_{\text{obsi}} - SS_{\text{prei}})^2}, \quad (17)$$

$$DC = 1 - \frac{\sum_{i=1}^N (SS_{\text{obsi}} - SS_{\text{prei}})^2}{\sum_{i=1}^N (SS_{\text{obsi}} - S_{\bar{S}_{\text{obs}}})^2}, \quad (18)$$

where  $SS_{\text{obsi}}$ ,  $SS_{\text{prei}}$ ,  $S_{\bar{S}_{\text{obs}}}$ , and  $N$  are observed, predicted, and average of the observed SSL values and number of observations, respectively.

### 3. Results and Discussion

All of the used models, namely, SVM, FFNN, ANFIS, and MLR, were trained and tested for modeling suspended sediment load in Katar catchment. The results of sensitivity analysis to select dominant inputs, single black-box modeling, and ensemble models for suspended sediment load are presented in the following subsections.

**3.1. Results of Inputs Selection.** The effect of several factors, for example, runoff, precipitation, and catchment characteristics, are involved in the suspended sediment load modeling [5]. Therefore, careful selection of the most relevant and significant factors as inputs in any AI-based modeling is an important step to obtain the optimum result. Previous studies indicated that there exists the highest correlation between the present value of suspended sediment load and its previous values. The influence of different factors can indirectly be considered by the antecedent SSL values [53]. To estimate the current SSL ( $SS_t$ ), different lag time series of discharge ( $Q$ ) and SSL were used in previous researches [4, 18]. Thus, the value of suspended sediment load at the current time step ( $SS_t$ ) would be the function of

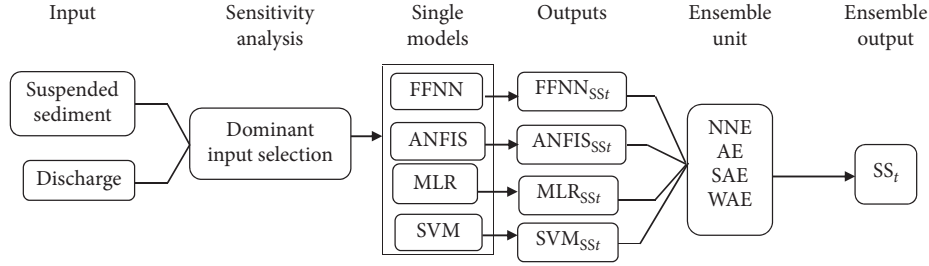


FIGURE 9: Schematic view of the ensemble process.

the sediment values up to time step  $n$  and also runoff ( $Q$ ) values at present and up to time step  $m$  as

$$SS_t = f(Q_t, Q_{t-1}, Q_{t-2}, \dots, Q_m, SS_{t-1}, SS_{t-2}, \dots, SS_n). \quad (19)$$

Selection of the most relevant input variables and correct network parameter adjustment (e.g., number of training iterations, hidden neurons, and transfer function) in any AI-based modeling is a crucial step in attaining the most optimal result [35, 54]. Linear sensitivity analysis methods (e.g., Pearson correlation) have previously been used for the selection of the dominant input variable in suspended sediment modeling (e.g., see [6, 21, 22, 55]). However, the application of linear Pearson correlation analysis for selecting the dominant input variables has been criticized by previous works (e.g., [35, 56]) since, for a complex nonlinear hydrological process like SSL, there may exist a stronger nonlinear relationship between the predictor and predicted variables than a weak linear relationship. Because of this, sensitivity analysis of input variables for suspended sediment load estimation using nonlinear FFNN was conducted in this work to determine the most relevant inputs. To predict current-day suspended sediment load ( $SS_t$ ), different lags (up to 5 past days) of suspended sediment and discharge data were evaluated as sole input and ranked based on the verification phase DC values of the modeling. The ranking results based on sensitivity analysis of input variables to predict  $SS_t$  are presented in Table 2.

In Table 2,  $t$  stands for the present time step and the corresponding output is the current suspended sediment load ( $SS_t$ ). In the table, the highest DC value implies the most dominant input variable. Thus,  $Q_t$  is the first most dominant and  $SS_{t-1}$  is the second, and  $Q_{t-1}$  is the third dominant input parameter. Insufficient input variables cannot give accurate results whereas including too many input variables makes the modeling process complex and may cause overfitting issues [35]. Thus, after ranking the input variables based on their verification DC value, the Student  $t$ -test was performed to identify the dominant inputs and remove those which do not have a significant impact on the estimation results. Based on the result of the Student  $t$ -test,  $Q_{t-4}$ ,  $Q_{t-5}$ ,  $SS_{t-4}$ , and  $SS_{t-5}$  were found less relevant and not included in the inputs combination set. After the selection of the dominant inputs and removal of less relevant inputs, different input combinations using the remaining parameters, that is,  $SS_{t-1}$ ,  $SS_{t-2}$ ,  $SS_{t-3}$ ,  $Q_t$ ,  $Q_{t-1}$ ,  $Q_{t-2}$ , and  $Q_{t-3}$ , were examined to predict the SSL by the proposed models.

TABLE 2: Sensitivity analysis results.

Inputs	Verification DC	Rank
$Q_t$	0.8208	1
$SS_{t-1}$	0.7964	2
$Q_{t-1}$	0.7605	3
$SS_{t-2}$	0.6338	4
$Q_{t-2}$	0.60438	5
$Q_{t-3}$	0.5188	6
$SS_{t-3}$	0.4966	7
$Q_{t-4}$	0.3594	8
$SS_{t-4}$	0.3027	9
$Q_{t-5}$	0.2934	10
$SS_{t-5}$	0.2134	11

**3.2. Results of SS Modeling Using Single Models.** For each input combination, the ANFIS, SVM, FFNN, and MLR models were trained and tested where the best results of each model are presented in Table 3. The FFNN model with five inputs and one hidden layer trained by the Levenberg-Marquardt algorithm was developed for suspended sediment load estimation in the Katar catchment. Determination of the optimal model structure (e.g., number of the hidden neurons) is an important step in FFNN modeling to obtain the best result. This is because too small neurons may capture unacceptable information while too many neurons may cause overfitting. A trial and error method by assessing the accuracy of different models trained with varying hidden neuron number was used to determine the best structure of the model. For the best input combination, 8 hidden neurons were found as the optimum structure of the hidden layer.

The second AI applied in this study was SVM. Radial basis function (RBF) kernel was used to create the SVM model for all input combinations. This kernel was selected because it provides better performance and contains fewer tuning parameters than polynomial and sigmoidal kernels [44].

The third AI-based model used was the ANFIS model that is known for its ability to handle the uncertainty of complex and nonlinear processes via a fuzzy concept. In this way for the ANFIS model, Sugeno fuzzy inference system using a hybrid algorithm was used to calibrate the MF parameters. The study also used a trial and error approach by changing the types of MFs to obtain the best result. Trapezoidal, triangular, and Gaussian-shaped MFs were examined because of their suitability in modeling the hydroclimatic process [25]. As well, the trial and error

TABLE 3: Results of single black-box models for SSL modeling by the best input combination.

Model	Input combination	Best structure	Training		Verification	
			DC	RMSE	DC	RMSE
FFNN	$Q_t, Q_{t-1}, Q_{t-2}, SS_{t-1}, SS_{t-2}$	5-8-1	0.876	0.03134	0.834	0.04155
ANFIS	$Q_t, Q_{t-1}, Q_{t-2}, SS_{t-1}, SS_{t-2}$	Gaussian	0.918	0.0255	0.884	0.0339
SVM	$Q_t, Q_{t-1}, Q_{t-2}, SS_{t-1}, SS_{t-2}$	RBF	0.867	0.0324	0.815	0.0439
MLR	$Q_t, Q_{t-1}, Q_{t-2}, SS_{t-1}, SS_{t-2}$	5-1	0.755	0.0441	0.708	0.0553

RMSE has no unit as the data are normalized.

method was used to determine the number of membership functions and to determine the best ANFIS construction. ANFIS model with Gaussian MFs trained by 55 epochs gave the best result among the others. Lastly, MLR that expresses the linear relationship between the predictor (independent) and output (dependent) variables was also applied for SSL modeling. The obtained results of the developed AI-based and MLR models to predicted suspended sediment load in Katar catchment for the best input combination are presented in Table 3. The numbering of a-b-c in the FFNN (Table 3) stands for the number of input, hidden, and output neuron layers. Similarly, the numbering y-z in the structure of MLR in Table 3 represents the number of inputs and output parameters.

Table 3 shows that the ANFIS model having the highest DC and lowest RMSE outperformed all developed AI and MLR models in suspended sediment load estimation followed by FFNN, SVM, and MLR. The result is confirmed by previous studies about the performance of ANFIS and ANN models in suspended sediment load estimation [12, 13]. The MLR which measures the linear relationship between the inputs and output led to less accurate results than the AI-based models. This is because the suspended sediment load is a dynamic, nonlinear, and complex process and hence a nonlinear model may be used to accurately model it instead of a linear technique.

From the results of single models shown in Table 4, the application of the best model (ANFIS) could increase the performances (based on DC value) of FNNN, SVM, and MLR by 6%, 8.47%, and 24.86%, respectively. In addition to statistical performance measures, different visual indicators like scatter plots, boxplot, and Taylor diagram were used in this study to obtain a better view of the estimation performances of the employed models. The scatter plots of single AI-based and MLR model result against the observed value in the verification phase are presented in Figure 10.

According to Sharafati et al. [31], a scatter plot shows the possible pattern similarity between the observed and estimated data. Figure 10 compares the estimation performance of FFNN, MLR, SVM, and ANFIS models in the estimation of SSL on scatter plots. The figure reveals less spread of points for predicted and observed SSL in the ANFIS model than other computing single models. This could be due to the ability of the ANFIS model to handle the uncertainties of the SSL process.

In Figure 11, the median ( $Q_{50\%}$ ) value for ANFIS model = 1,497.3 ton/day, MLR = 2014.4 ton/day, SVM = 1,672.7, FFNN = 1,562.8 ton/day, and observed = 1,482 ton/day. This indicates the ANFIS model performs better than

the other models with FFNN being the second while MLR provides the worst estimation. The reasonable performance of the ANFIS model is because of its ability to handle the uncertainty of complex SSL process. Kumar et al. [12] applied ANFIS and ANN to model the current-day suspended sediment and runoff in the Godavari basin using the previous period discharge and SSL data as input. They found that the ANFIS model gave a better performance than ANN in suspended sediment prediction. Nourani and Andalib [4] employed the least squares support vector regression (LSSVR) and ANN for monthly and daily SSL prediction. The result showed that LSSVR has a better predictive performance than ANN. Buyukyildiz and Kumcu [18] applied SVM, ANFIS, and SVM to estimate the current-day SSL of Coruh River using a different combination of lag time series of Q and SSL as input. They found that ANN performed better than the other models. From the comparison with the reported studies in the literature, it can be observed that the estimation accuracy of AI-based models varies for different case studies. According to Salih et al. [2], it is because of SSL data stochasticity of each considered catchment and also the capacity of the constructed AI-based models to handle the nonstationarity and nonlinearity in the data set.

Figure 12(a) shows the time series plot of observed versus computed suspended sediment load in the verification phase of Abura station for the applied MLR, SVM, FFNN, and ANFIS models. Figure 12(b) shows a section of modeling of SSL time series by MLR, SVM, FFNN, and ANFIS models. For better visibility of predicted values of SSL by each model, only a 51-day period (from July 26 to September 14, 2017) has been focused on in Figure 12(b).

As shown in Figure 12(b), the date of July 29, August 08, August 24, and August 31 are marked as points 1, 2, 3, and 4, respectively. With regard to point 1, ANFIS = 5752.136 ton/day, MLR = 3857.018 ton/day, FFNN = 4620.326 ton/day, SVM = 6573.967 ton/day, and observed = 3831.348 ton/day. This indicates that the MLR value is more close to the actual value than the other models. This, in turn, shows that even the least accurate model at a certain point in the time series could give the best result. With regard to point 2, ANFIS = 6313.366 ton/day, MLR = 4563.506 ton/day, SVM = 8595.878 ton/day, FFNN = 6695.642 ton/day, and observed = 6245.252 ton/day. This implies that the ANFIS model performs better than other models. At point 3, ANFIS = 6181.81 ton/day, MLR = 4190.825 ton/day, SVM = 6270.75 ton/day, FFNN = 5424.629 ton/day, and observed = 5249.579 ton/day. This indicates that the FFNN value has less deviation from the observed SSL value than the other competing models. At the final point (point 4), SVM

TABLE 4: Results of the proposed ensemble methods for SSL modeling.

Ensemble method	Best structure	Calibration		Verification	
		DC	RMSE	DC	RMSE
SAE	4-1	0.922	0.0249	0.8793	0.0349
WAE	0.257, 0.274, 0.251, 0.218	0.9257	0.0243	0.888	0.0327
AE	Gaussian-3	0.9804	0.0125	0.97	0.0176
NNE	4-7-1	0.953	0.0193	0.924	0.0281

RMSE has no unit as the data used is normalized.

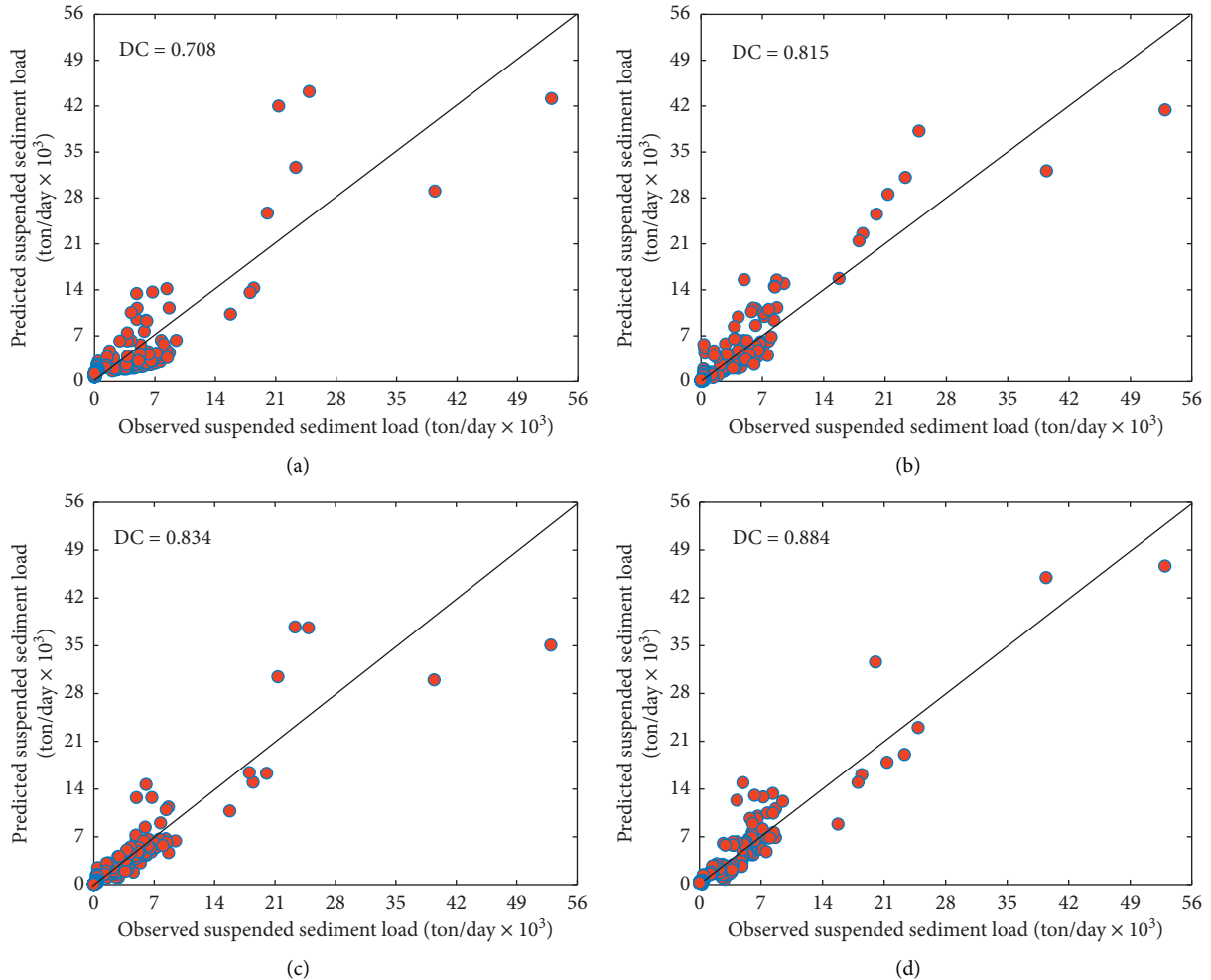


FIGURE 10: Scatter plots showing the actual and predicted SSL, at verification phase by (a) MLR, (b) SVM, (c) FFNN, and (d) ANFIS.

performs better than the other models. From the results of the selected points, it is clear that different models at different time points could lead to different performances (from different data aspects). Thus, the objective of more accurate SSL estimation can be better achieved through an ensemble method. In this regard, WAE, SAE, NNE, and AE ensemble methods were developed for SSL modeling to improve the overall performance of the modeling.

**3.3. Results of Ensemble Techniques.** In order to increase the estimation efficiency of single AI-based and MLR models, the outputs of ANFIS, SVM, MLR, and FFNN models were

used as inputs for the four ensemble techniques as a novel ensemble method for SSL modeling. The results of linear and nonlinear ensemble models for suspended sediment estimation are presented in Table 4.

Table 4 shows the performances of WAE, SAE, AE, and NNE for the estimation of SSL. In the SAE structure, a-b is used to show the number of inputs and outputs (SSt). In WAE structure,  $w$ ,  $x$ ,  $y$ , and  $z$  denote the weights of FFNN, ANFIS, SVM, and MLR models, respectively. In Table 4, it can be seen that AE outperformed all the competing model combination techniques because of its robustness by combining the advantages of both ANN and fuzzy concepts via the ANFIS framework.

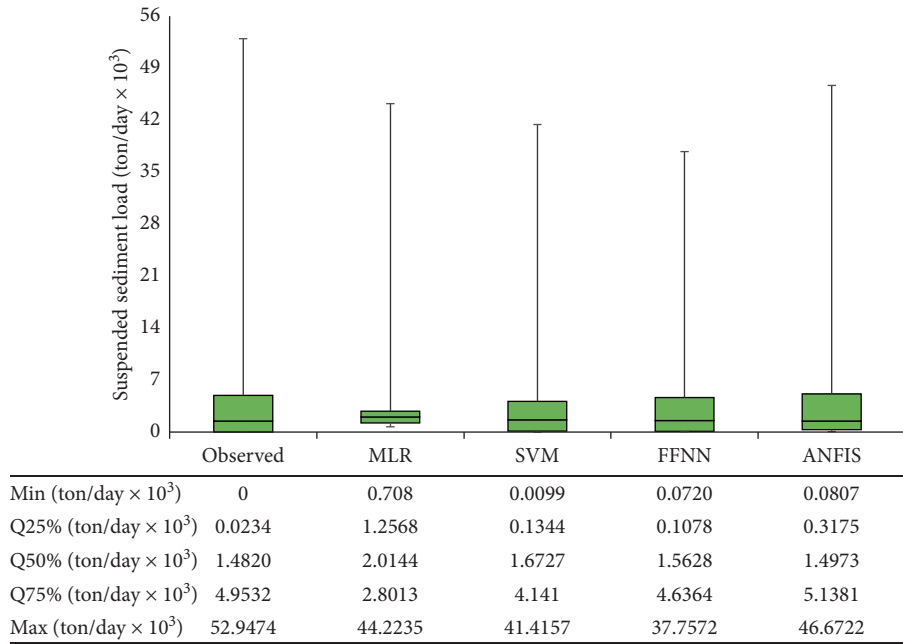


FIGURE 11: Boxplot of observed versus computed SSL in the verification phase.

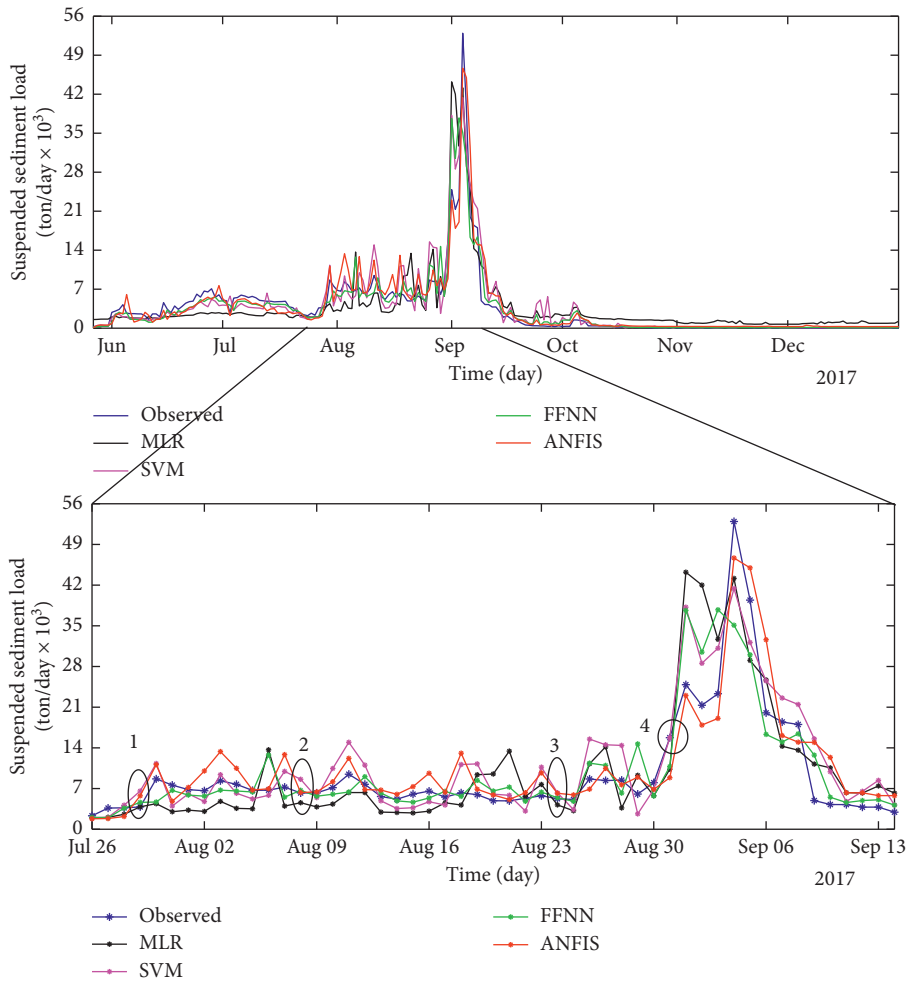


FIGURE 12: Observed versus predicted suspended sediment load value in the verification stage of Abura station in (a) January 2016–December 2019 and (b) July 26 up to September 14, 2017.

The linear ensemble (SAE) performed better than all the single models except the ANFIS model. It is known that linear averaging usually gives values higher than the minimum value and lesser than the highest value in the data set [35]. Even from the nonlinear ensemble methods, WAE gives a slightly better performance than SAE. This could be due to the assigned weights on the parameter based on their relative importance.

NNE model was trained by the Levenberg-Marquardt algorithm similar to the single FFNN model and the tangent sigmoid activation function was utilized for both output and hidden layers. In this study, the Levenberg-Marquardt algorithm was selected among different ANN training algorithms because of its fastest convergence ability as reported by Sahoo et al [57]. A trial and error process was used to determine the best epoch number and the appropriate number of hidden neurons. NNE has been successfully used as multimodel combination techniques in hydrological modeling (e.g., [25, 46, 52]). Similar to the ANFIS single model, Sugeno fuzzy inference system using a hybrid training algorithm was used to calibrate the MFs parameters in AE. The AE model has greatly enhanced the accuracy of single models in previous studies in another field [35].

The result in Table 5 shows the capability of ensemble techniques to improve the prediction performance of single AI and MLR models based on their DC values. The results in Table 5 show that all used ensemble methods can be applied to improve single model performance in SSL modeling. However, nonlinear ensemble techniques show superiority over the linear ensemble models. This could be because of the incapability of linear ensemble methods to undergo another black-box learning process unlike the nonlinear ensemble methods (AE and NNE). The NNE increased the performance of SVM, FFNN, ANFIS, and MLR models by 12%, 12.8%, 6.6%, and 28.4%, respectively in the verification stage. In the AE model, the performance of SVM, FFNN, ANFIS, and MLR models was increased by 16.4%, 17.3%, 10.9%, and 33.5%, respectively, in the verification stage. Also, from the obtained results shown in Table 4, the AE performed better than the other three ensemble methods because of its robustness to handle the complex nonlinear process between outputs and inputs. The performance accuracy of the ANFIS model over AI-based and MLR single models applied in modeling suspended sediment load was also confirmed by the AE model.

The scatter plots of the ensemble methods result and the observed suspended sediment load values in the verification phase are presented in Figure 13.

In Figure 13, the scatter plots of the developed ensemble models for SSL estimation in the verification are compared. As indicated in the figure, the AE is seen to have less spread estimation and the points were closer to the best line compared to the other ensemble models, while the linear ensemble methods (SAE and WAE) show the most scattered estimation.

TABLE 5: The comparison of the nonlinear ensemble models using single AI and MLR models.

Model	Training (%)	Verification (%)
AE vs MLR	29.85	37
AE vs FFNN	11.9	16.3
AE vs SVM	13.08	19.02
AE vs ANFIS	6.8	9.73
NNE vs MLR	26.22	30.5
NNE vs SVM	9.92	13.37
NNE vs FFNN	8.8	10.79
NNE vs ANFIS	3.8	4.5

The boxplot is also another graph commonly used to make a comparison between the observed value and estimated outputs obtain by different models [6, 31]. The variability of observed SSL values versus those obtained by the developed ensemble models was compared using different quartiles and interquartile range (IQR) through boxplots in Figure 14. In this figure, the median ( $Q_{50\%}$ ) value for SAE = 1,681.1 ton/day, WAE = 1, 678 ton/day, NNE = 1,212.4 ton/day, AE = 1,636.4 ton/day, and observed = 1, 482 ton/day. This shows that AE outperforms the other ensemble techniques. Moreover, Figure 14 depicts that the most consistency is found between the output obtained by AE (IQR = 4,968.3 ton/day) and observed value (IQR = 4,929.8 ton/day).

Figure 15 shows the time series of observed versus predicted SSL in the verification phase of Abura station SSL modeling for the applied ensemble methods (SAE, WAE, NNE, and AE). From Figure 15, it is clear that the WAE and SAE methods were less accurate than AE and NNE. The values of AE were more fitted with the observed data, whereas there is a wider fluctuation between observed data and the values obtained by WAE and SAM ensembles.

Alternatively, four ensemble methods (SAE, WAE, AE, and NNE) were also assessed using the Taylor diagram (two-dimensional diagram), which shows the predicted and observed values. Taylor's diagram could be used as a successful diagram for comparison of model performances in different fields [2, 6, 58–60]. Taylor's diagram was used to construct and graphically visualize the combination of two performance indicators, namely, correlation ( $r$ ) and standard deviation (SD) [61] (Figure 16). The key objective of using this diagram is to combine different models performances indicators in one graph and it can also statistically quantify the level of resemblance between the predicted and observed values. From Figure 16, it is seen that the best ensemble method is AE ( $r=0.985$ ) and SAE is the least with the  $r$ -value of 0.927. From the ensemble result comparisons, the mentioned performance metrics indicate the degree of prediction accuracy of AE. The AE outperformed the other ensemble methods as the predicted values are more close to the observed values. This can be additionally confirmed by considering the high SD value which could be credited to the AE.

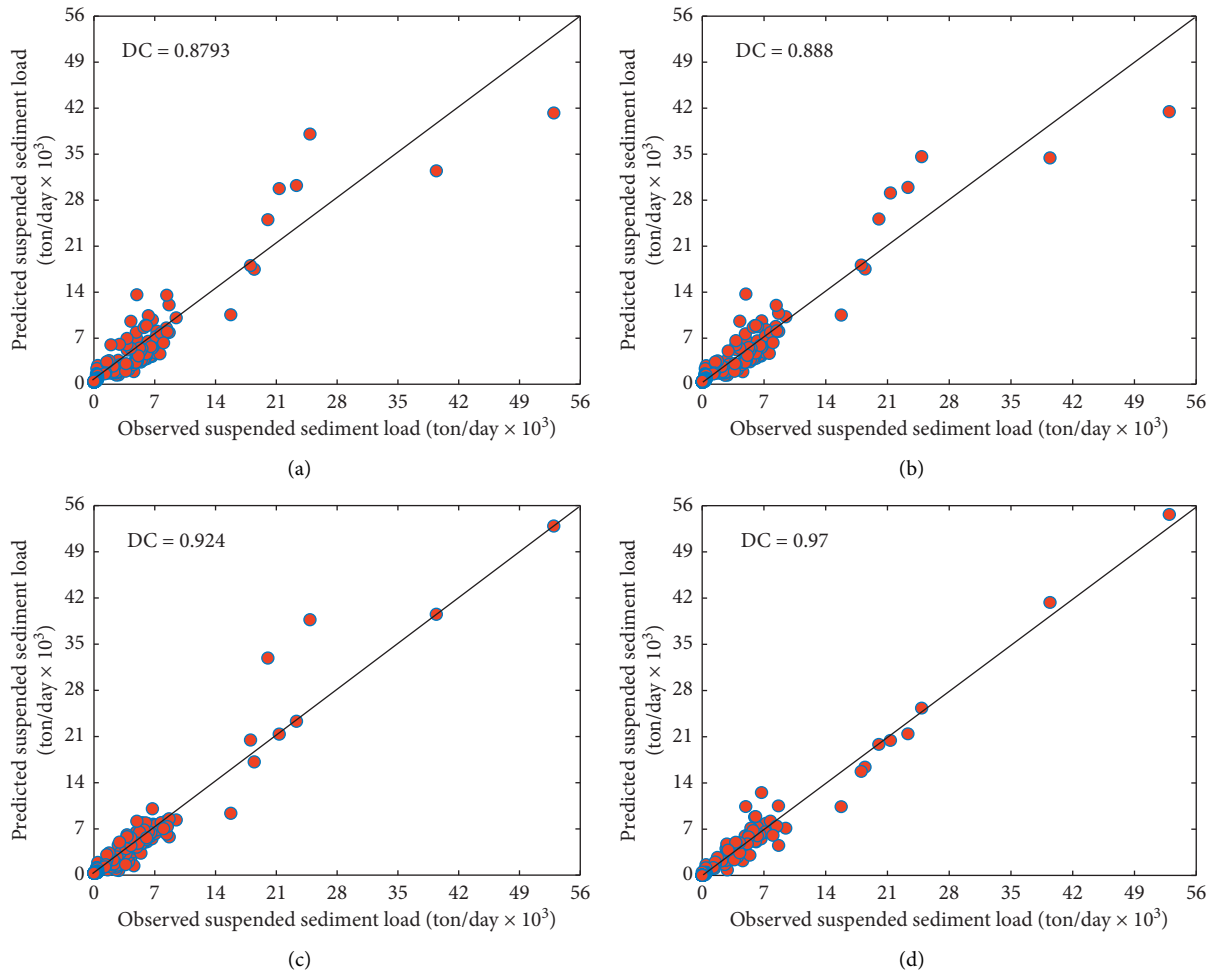


FIGURE 13: Scatter plots showing observed versus predicted suspended sediment load by (a) SAE, (b) WAE, (c) NNE, and (d) AE, in the verification phase.

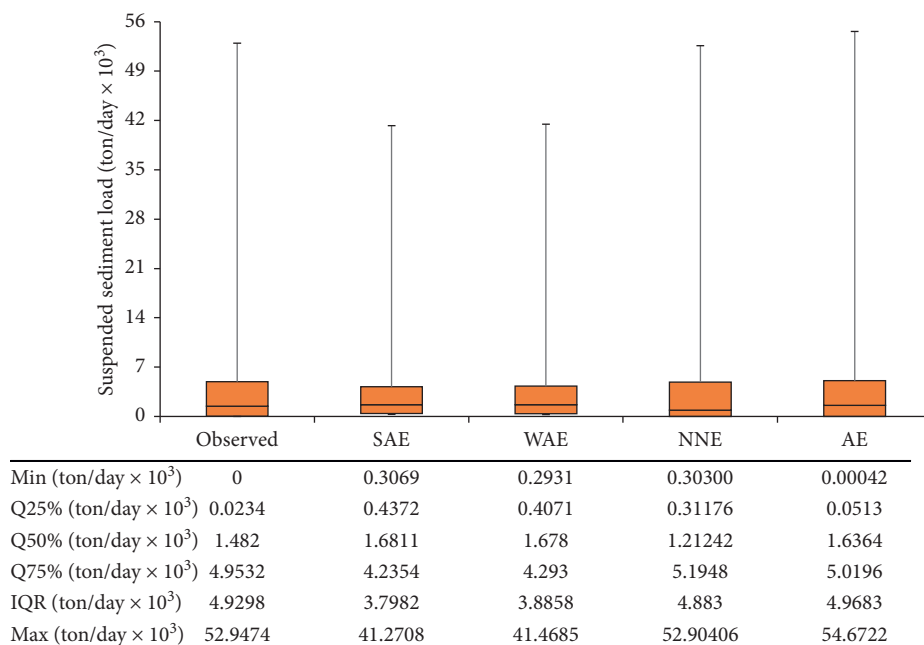


FIGURE 14: Boxplot of observed versus predicted values by ensemble models in the verification phase.

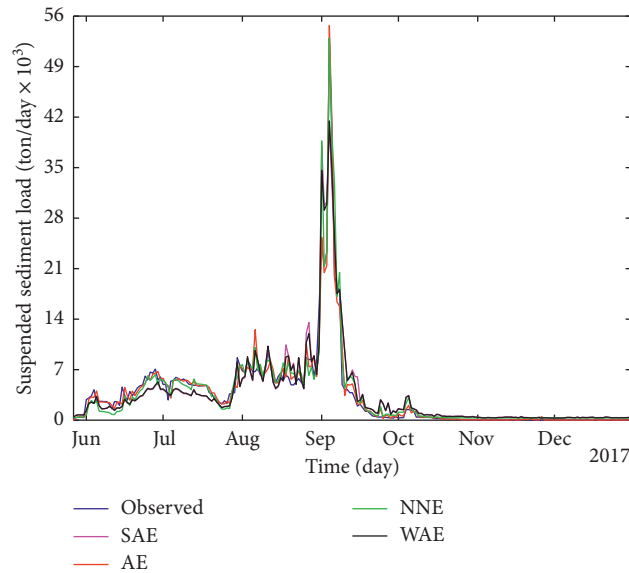


FIGURE 15: Time series of the observed versus ensemble models value in the verification phase.

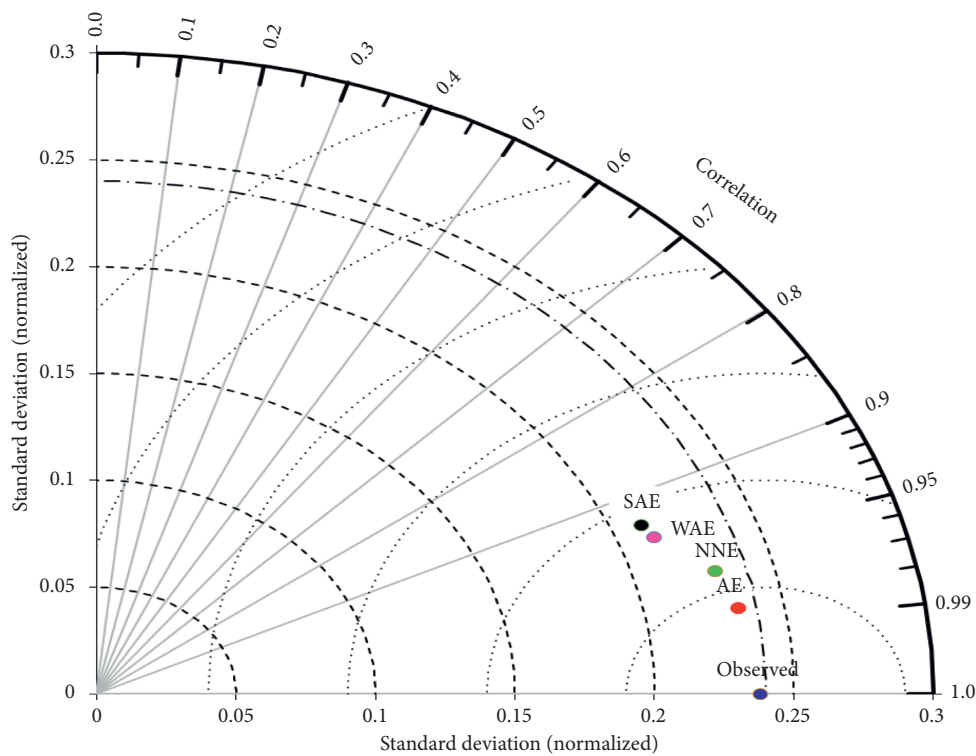


FIGURE 16: Normalized Taylor diagram showing the performance of ensemble models.

#### 4. Conclusions

In this study, the capability of ANFIS, SVR, FFNN, and MLR models was examined for modeling daily SSL of Katar catchment, Ethiopia. Before the development of suspended sediment load estimation using single AI and MLR models, a nonlinear sensitivity analysis was conducted for selecting the relevant inputs. After conducting the Student *t*-test, some irrelevant and less significant input variables were removed

and only the dominant inputs were used in different combinations to predict SSL.

By comparing the results obtained from the single models, it was demonstrated that the ANFIS model could lead to the highest prediction performance over the other competing models because of its strength in dealing with the dynamic, nonlinear, and complex process via fuzzy concept. After developing single AI and conventional MLR models, four ensemble methods that combine the outputs from every



single back box models were created to improve the performances of the individual models. Combining the results of individual models enhanced the accuracy of single models in the estimation of suspended sediment. Nonlinear ensemble techniques (AE and NNE) showed the highest performance because of their capability of handling the uncertainty of complex and nonstationary processes such as the suspended sediment process. AE method showed superiority over the other ensemble methods by increasing the predictive performance of FFNN, ANFIS, MLR, and SVM models in the testing phase by 16.3%, 9.73%, 37%, and 19.02%, respectively. The performance of the nonlinear ensemble (SAE) showed higher efficiency compared to the single black-box models except the ANFIS model. This is because linear averaging always gives a result that is higher than the minimum value and lesser than the maximum value in the set. In this study, the linear ensemble provides less performance than the ANFIS model because of the lower performance of the conventional MLR. Therefore, the limitation of the linear ensemble method is that the least performed single models may lead to performance lower than that of the most accurate model.

The result of this study generally revealed the promising power of ensemble methods in SSL modeling. The ensemble outputs obtained specifically by the AE technique revealed that better SSL forecasting accuracy could be achieved via a combination of individual model outputs rather than the use of single models. This study is limited to the application of black-box models for ensemble SSL modeling. Hence, the inclusion of physically based models in the ensemble unit should be tested for future study. Moreover, this study used only two years of daily SSL and discharge data for suspended sediment load estimation due to the data limitation. Thus, more data and input parameters can be tested for future studies.

## Data Availability

Data are available from the corresponding author upon request.

## Conflicts of Interest

The authors declare no conflicts of interest.

## References

- [1] O. Kisi, A. H. Dailr, M. Cimen, and J. Shiri, "Suspended sediment modeling using genetic programming and soft computing techniques," *Journal of Hydrology*, vol. 450-451, pp. 48-58, 2012.
- [2] S. Q. Salih, A. Sharafati, K. Khosravi et al., "River suspended sediment load prediction based on river discharge information: application of newly developed data mining models," *Hydrological Sciences Journal*, vol. 65, no. 4, pp. 624-637, 2020.
- [3] C. G. Liu, Z. Y. Li, Y. Hao, J. Xia, F. W. Bai, and M. A. Mehmood, "Computer simulation elucidates yeast flocculation and sedimentation for efficient industrial fermentation," *Biotechnology Journal*, vol. 13, no. 5, pp. 1-7, 2018.
- [4] V. Nourani and G. Andalib, "Daily and monthly suspended sediment load predictions using wavelet based artificial intelligence approaches," *Journal of Mountain Science*, vol. 12, no. 1, pp. 85-100, 2015.
- [5] V. Nourani, A. Molajou, A. D. Tajbakhsh, and H. Najafi, "A wavelet based data mining technique for suspended sediment load modeling," *Water Resources Management*, vol. 33, no. 5, pp. 1769-1784, 2019.
- [6] A. Sharafati, S. B. Haji Seyed Asadollah, D. Motta, and Z. M. Yaseen, "Application of newly developed ensemble machine learning models for daily suspended sediment load prediction and related uncertainty analysis," *Hydrological Sciences Journal*, vol. 65, no. 12, pp. 1-21, 2020.
- [7] M. J. Alizadeh, E. Jafari Nodoushan, N. Kalarestaghi, and K. W. Chau, "Toward multi-day-ahead forecasting of suspended sediment concentration using ensemble models," *Environmental Science and Pollution Research*, vol. 24, no. 36, pp. 28017-28025, 2017.
- [8] T. Abebe and B. Gebremariam, "Modeling runoff and sediment yield of kesem dam watershed, awash basin, Ethiopia," *SN Applied Sciences*, vol. 1, no. 5, pp. 1-13, 2019.
- [9] G. D. Betrie, Y. A. Mohamed, A. Van Griensven, and R. Srinivasan, "Sediment management modelling in the blue Nile basin using SWAT model," *Hydrology and Earth System Sciences*, vol. 15, no. 3, pp. 807-818, 2011.
- [10] A. Martínez-Salvador and C. Conesa-García, "Suitability of the SWAT model for simulating water discharge and sediment load in a karst watershed of the semiarid mediterranean basin," *Water Resources Management*, vol. 34, pp. 85-802, 2020.
- [11] B. Sivakumar, "Suspended sediment load estimation and the problem of inadequate data sampling: a fractal view," *Earth Surface Processes and Landforms*, vol. 31, no. 4, pp. 414-427, 2006.
- [12] A. Kumar, P. Kumar, and V. K. Singh, "Evaluating different machine learning models for runoff and suspended sediment simulation," *Water Resources Management*, vol. 33, no. 3, pp. 1217-1231, 2019.
- [13] E. Olyaie, H. Banejad, K. W. Chau, and A. M. Melesse, "A comparison of various artificial intelligence approaches performance for estimating suspended sediment load of river systems: a case study in the United States," *Environmental Monitoring and Assessment*, vol. 187, no. 4, 2015.
- [14] O. Kisi, J. Shiri, and M. Tombul, "Modeling rainfall-runoff process using soft computing techniques," *Computers & Geosciences*, vol. 51, pp. 108-117, 2013.
- [15] R. M. Adnan, A. Petroselli, S. Heddham, C. A. G. Santos, and O. Kisi, "Short term rainfall-runoff modeling using several machine learning methods and a conceptual event-based model," *Stochastic Environmental Research and Risk Assessment*, pp. 1-20, 2020.
- [16] F. Saberi-Movahed, M. Najafzadeh, and A. Mehrpooya, "Receiving more accurate predictions for longitudinal dispersion coefficients in water pipelines: training group method of data handling using extreme learning machine conceptions," *Water Resources Management*, vol. 34, no. 2, pp. 529-561, 2020.
- [17] M. Najafzadeh and G. Oliveto, "Riprap incipient motion for overtopping flows with machine learning models," *Journal of Hydroinformatics*, vol. 22, no. 4, pp. 749-767, 2020.
- [18] M. Buyukyildiz and S. Y. Kumcu, "An estimation of the suspended sediment load using adaptive network based fuzzy inference system, support vector machine and artificial neural

- network models,” *Water Resources Management*, vol. 31, no. 4, pp. 1343–1359, 2017.
- [19] H. A. Afan, A. El-Shafie, Z. M. Yaseen, M. M. Hameed, W. H. M. Wan Mohtar, and A. Hussain, “ANN based sediment prediction model utilizing different input scenarios,” *Water Resources Management*, vol. 29, no. 4, pp. 1231–1245, 2014.
- [20] A. M. Melesse, S. Ahmad, M. E. McClain, X. Wang, and Y. H. Lim, “Suspended sediment load prediction of river systems: an artificial neural network approach,” *Agricultural Water Management*, vol. 98, no. 5, pp. 855–866, 2011.
- [21] T. Rajaei, V. Nourani, M. Zounemat-Kermani, and O. Kisi, “River suspended sediment load prediction: application of ANN and wavelet conjunction model,” *Journal of Hydrologic Engineering*, vol. 17, no. 5, pp. 604–614, 2011.
- [22] E. K. Lafdani, A. M. Nia, and A. Ahmadi, “Daily suspended sediment load prediction using artificial neural networks and support vector machines,” *Journal of Hydrology*, vol. 478, pp. 50–62, 2013.
- [23] H. Tabari, O. Kisi, A. Ezani, and P. Hosseinzadeh Talaei, “SVM, ANFIS, regression and climate based models for reference evapotranspiration modeling using limited climatic data in a semi-arid highland environment,” *Journal of Hydrology*, vol. 444, no. 445, pp. 78–89, 2012.
- [24] R. Ampomah, H. Hosseiny, L. Zhang, V. Smith, and K. Sample-Lord, “A regression-based prediction model of suspended sediment yield in the cuyahoga river in Ohio using historical satellite images and precipitation data,” *Water (Switzerland)*, vol. 12, no. 3, 2020.
- [25] V. Nourani, G. Elkiran, and J. Abdullahi, “Multi-step ahead modeling of reference evapotranspiration using a multi-model approach,” *Journal of Hydrology*, vol. 581, Article ID 124434, 2020.
- [26] A. Y. Shamseldin, K. M. O’Connor, and G. C. Liang, “Methods for combining the outputs of different rainfall-runoff models,” *Journal of Hydrology*, vol. 197, no. 1–4, pp. 203–229, 1997.
- [27] J. M. Bates and C. W. J. Granger, “The combination of forecasts,” *Journal of the Operational Research Society*, vol. 20, no. 4, pp. 451–468, 1969.
- [28] R. N. Kiran and V. Ravi, “Software reliability prediction by soft computing techniques,” *Journal of Systems and Software*, vol. 81, no. 4, pp. 576–583, 2008.
- [29] S. Makridakis, A. Andersen, R. Carbone et al., “The accuracy of extrapolation (time series) methods: results of a forecasting competition,” *Journal of Forecasting*, vol. 1, no. 2, pp. 111–153, 1982.
- [30] S. B. H. S. Asadollah, A. Sharafati, D. Motta, and Z. M. Yaseen, “river water quality index prediction and uncertainty analysis: a comparative study of machine learning models,” *Journal of Environmental Chemical Engineering*, vol. 9, no. 1, Article ID 104599, 2020.
- [31] A. Sharafati, S. B. H. S. Asadollah, and M. Hosseinzadeh, “The potential of new ensemble machine learning models for effluent quality parameters prediction and related uncertainty,” *Process Safety and Environmental Protection*, vol. 140, pp. 68–78, 2020.
- [32] G. Cavadias and G. Morin, “The combination of simulated discharges of hydrological models,” *Hydrology Research*, vol. 17, no. 1, pp. 21–32, 1986.
- [33] V. Nourani, G. Elkiran, and J. Abdullahi, “Multi-station artificial intelligence based ensemble modeling of reference evapotranspiration using Pan evaporation measurements,” *Journal of Hydrology*, vol. 577, Article ID 123958, 2019.
- [34] A. Sharafati, S. B. H. S. Asadollah, and A. Neshat, “A new artificial intelligence strategy for predicting the groundwater level over the Rafsanjan aquifer in Iran,” *Journal of Hydrology*, vol. 591, Article ID 125468, 2020.
- [35] V. Nourani, H. Gökçekuş, and I. K. Umar, “Artificial intelligence based ensemble model for prediction of vehicular traffic noise,” *Environmental Research*, vol. 180, Article ID 108852, 2020.
- [36] A. Aga, A. Melesse, and B. Chane, “Estimating the sediment flux and budget for a data limited rift valley lake in Ethiopia,” *Hydrology*, vol. 6, no. 1, p. 1, 2018.
- [37] R. Tanty and T. S. Desmukh, “Application of artificial neural network in hydrology—a review,” *International Journal of Engineering and Technical Research*, vol. 4, no. 6, 2015.
- [38] J.-S. R. Jang, “ANFIS: adaptive-network-based fuzzy inference system,” *IEEE Transactions on Systems, Man, and Cybernetics*, vol. 23, no. 3, pp. 665–685, 1993.
- [39] J. S. R. Jang, C. T. Sun, and E. Mizutani, *Neuro-Fuzzy and Soft Computing—A Computational Approach to Learning and Machine Intelligence*, Prentice Hall, Trenton, NJ, USA, 1997.
- [40] Y. Tsukamoto, “An approach to fuzzy reasoning method,” *Advances in Fuzzy Set Theory and Applications*, vol. 137, no. 149, 1979.
- [41] T. Takagi and M. Sugeno, “Fuzzy identification of systems and its applications to modeling and control,” *IEEE Transactions on Systems, Man, and Cybernetics*, vol. SMC-15, no. 1, pp. 116–132, 1985.
- [42] E. H. Mamdani and S. Assilian, “An experiment in linguistic synthesis with a fuzzy logic controller,” *International Journal of Man-Machine Studies*, vol. 7, no. 11, pp. 1–13, 1975.
- [43] A. M. Kalteh, “Monthly river flow forecasting using artificial neural network and support vector regression models coupled with wavelet transform,” *Computers & Geosciences*, vol. 54, pp. 1–8, 2013.
- [44] W.-C. Wang, D.-M. Xu, K.-W. Chau, and S. Chen, “Improved annual rainfall-runoff forecasting using PSO-SVM model based on EEMD,” *Journal of Hydroinformatics*, vol. 15, no. 4, pp. 1377–1390, 2013.
- [45] A. H. Haghiabi, H. M. Azamathulla, and A. Parsaie, “Prediction of head loss on cascade weir using ANN and SVM,” *ISH Journal of Hydraulic Engineering*, vol. 23, no. 1, pp. 102–110, 2017.
- [46] E. Sharghi, V. Nourani, and N. Behfar, “Earthfill dam seepage analysis using ensemble artificial intelligence based modeling,” *Journal of Hydroinformatics*, vol. 20, no. 5, pp. 1071–1084, 2018.
- [47] V. Nourani, G. Elkiran, and S. I. Abba, “Wastewater treatment plant performance analysis using artificial intelligence—an ensemble approach,” *Water Science and Technology*, vol. 78, no. 10, 2018.
- [48] P. Kazienko, E. Lughofer, and B. Trawiński, “Hybrid and ensemble methods in machine learning J.UCS special issue,” *Journal of Universal Computer Science*, vol. 19, no. 4, pp. 457–461, 2013.
- [49] N. K. Ajami, Q. Duan, X. Gao, and S. Sorooshian, “Multi-model combination techniques for analysis of hydrological simulations: application to distributed model intercomparison project results,” *Journal of Hydrometeorology*, vol. 7, no. 4, pp. 755–768, 2006.
- [50] S. I. Abba, N. T. T. Linh, J. Abdullahi et al., “Hybrid machine learning ensemble techniques for modeling dissolved oxygen concentration,” *IEEE Access*, vol. 8, pp. 157218–157237, 2020.
- [51] C. W. Dawson, R. J. Abraham, and L. M. See, “HydroTest: a web-based toolbox of evaluation metrics for the standardised

- assessment of hydrological forecasts,” *Environmental Modelling & Software*, vol. 22, no. 7, pp. 1034–1052, 2007.
- [52] G. Elkiran, V. Nourani, S. I. Abba, and J. Abdullahi, “Artificial intelligence-based approaches for multi-station modelling of dissolve oxygen in river,” *Global Journal of Environmental Science and Management*, vol. 4, no. 4, pp. 439–450, 2018.
- [53] T. Partal and H. K. Cigizoglu, “Estimation and forecasting of daily suspended sediment data using wavelet-neural networks,” *Journal of Hydrology*, vol. 358, no. 3-4, pp. 317–331, 2008.
- [54] E. Sharghi, V. Nourani, H. Najafi, and H. Gokcekus, “Conjunction of a newly proposed emotional ANN (EANN) and wavelet transform for suspended sediment load modeling,” *Water Supply*, vol. 19, no. 6, pp. 1726–1734, 2019.
- [55] S. K. Himanshu, A. Pandey, and B. Yadav, “Ensemble wavelet-support vector machine approach for prediction of suspended sediment load using hydrometeorological data,” *Journal of Hydrologic Engineering*, vol. 22, no. 7, Article ID 05017006, 2017.
- [56] V. Nourani, K. T. Rezapour, and H. Baghanam, “Case studies in intelligent computing,” in *Case Studies in Intelligent Computing*, N. Issac and B. Israr, Eds., Taylor and Francis Group, New York, NY, USA, 2014.
- [57] G. B. Sahoo, C. Ray, and H. F. Wade, “Pesticide prediction in ground water in North Carolina domestic wells using artificial neural networks,” *Ecological Modelling*, vol. 183, no. 1, pp. 29–46, 2005.
- [58] G. Elkiran, V. Nourani, and S. I. Abba, “Multi-step ahead modelling of river water quality parameters using ensemble artificial intelligence-based approach,” *Journal of Hydrology*, vol. 577, Article ID 123962, 2019.
- [59] S. J. Hadi, S. I. Abba, S. S. Sammen, S. Q. Salih, N. Al-Ansari, and Z. M. Yaseen, “Non-linear input variable selection approach integrated with non-tuned data intelligence model for streamflow pattern simulation,” *IEEE Access*, vol. 7, pp. 141533–141548, 2019.
- [60] V. Nourani, H. Gökçekuş, I. K. Umar, and H. Najafi, “An emotional artificial neural network for prediction of vehicular traffic noise,” *Science of the Total Environment*, vol. 707, 2020.
- [61] K. E. Taylor, “Summarizing multiple aspects of model performance in a single diagram,” *Journal of Geophysical Research: Atmospheres*, vol. 106, pp. 7183–7192, 2001.